The Journal of Experimental Biology 212, 1990-1994
Published by The Company of Biologists 2009
doi:10.1242/jeb.028282

Spider silk as a novel high performance biomimetic muscle driven by humidity

Ingi Agnarsson[1,3], Ali Dhinojwala[2], Vasav Sahni[2] and Todd A. Blackledge[1,*]

[1]Department of Biology and [2]Department of Polymer Science, Integrated Bioscience Program, The University of Akron, Akron, OH 44325, USA and [3]Department of Biology, University of Puerto Rico, San Juan, PR 00931, USA

*Author for correspondence (e-mail: blackledge@uakron.edu)

Accepted 15 April 2009

SUMMARY

The abrupt halt of a bumble bee's flight when it impacts the almost invisible threads of an orb web provides an elegant example of the amazing strength and toughness of spider silk. Spiders depend upon these properties for survival, yet the impressive performance of silk is not limited solely to tensile mechanics. Here, we show that silk also exhibits powerful cyclic contractions, allowing it to act as a high performance mimic of biological muscles. These contractions are actuated by changes in humidity alone and repeatedly generate work 50 times greater than the equivalent mass of human muscle. Although we demonstrate that this response is general and occurs weakly in diverse hydrophilic materials, the high modulus of spider silk is such that it generates exceptional force. Furthermore, because this effect already operates at the level of single silk fibers, only 5 μm in diameter, it can easily be scaled across the entire size range at which biological muscles operate. By contrast, the most successful synthetic muscles developed so far are driven by electric voltage, such that they cannot scale easily across large ranges in cross-sectional areas. The potential applicability of silk muscles is further enhanced by our finding that silkworm fibers also exhibit cyclic contraction because they are already available in commercial quantities. The simplicity of using wet or dry air to drive the biomimetic silk muscle fibers and the incredible power generated by silk offer unique possibilities in designing lightweight and compact actuators for robots and micro-machines, new sensors, and green energy production.

Key words: supercontraction, major ampullate silk, biomaterial, *Nephila clavipes*.

INTRODUCTION

Most of the world's 40,000 species of spiders produce dragline silk from major ampullate silk glands to spin lifelines and frames of webs (Fig. 1A,B). Dragline silk's impressive toughness (work/volume ~5× greater than Kevlar®), high strength to weight ratio (~5× greater than steel), immunological compatibility with living tissue, and production under environmentally benign conditions all make spider silk an important model for biomimetic research (Gosline et al., 1986; Vadlamudi, 1995; Vollrath and Knight, 2001; Vollrath and Porter, 2006). Many of these properties result from the structure of silk proteins, which combine β-sheet crystals that interlock molecules together and stiffen fibers with less organized 'amorphous' regions of the proteins that allow molecular mobility (Gosline et al., 1999; Hayashi et al., 1999; Termonia, 1994). This composite structure results in fibers that are both strong and stretchy and that resist crack propagation. Spiders depend upon these properties for survival, yet the impressive performance of silk is not limited solely to tensile mechanics. Here, we show that spider silk also exhibits powerful cyclic contractions that are precisely controlled by changes in humidity, allowing silk to act as a high performance mimic of biological muscles.

At high humidity spider dragline silk 'supercontracts' – unrestrained silk will shrink up to 50% in length whereas restrained silk generates stresses in excess of 50 MPa (Bell et al., 2002; Guinea et al., 2003; Work, 1977). Water infiltrates the silk, disrupting hydrogen bonding within the amorphous region of the proteins (Jelinski et al., 1999; Schafer et al., 2008). This increases molecular mobility such that entropy can drive the proteins into a less organized configuration (Gosline et al., 1984). Supercontraction generates substantial forces providing the tantalizing possibility that the phenomenon could be exploited to perform work. However, such applicability is limited because supercontraction occurs in the silk of only some spiders, it is a one-time response, and it depends upon high molecular orientation to generate the initial low entropy state.

There are several other intriguing examples of materials in nature that move in response to humidity and that could provide inspiration for biomimetic muscle. The cellulose fibrils in wheat awns expand and contract in response to humidity, driving the wheat grains into the soil (Elbaum et al., 2007). The scales of seed-bearing pine cones open in response to humidity, helping to expel seeds (Dawson et al., 1997). Some synthetic materials can also change size when exposed to water or humidity (Beebe et al., 2000; Tanaka et al., 1980). These materials are all hydrophilic suggesting the hypothesis that movement is caused simply by swelling during bulk uptake of water. Here, for the first time, we show that spider dragline silk exhibits a similar, cyclic response to humidity, and demonstrate how that response can be harnessed to create precisely controlled biomimetic muscles for different applications.

MATERIALS AND METHODS

To examine the interaction of water with spider dragline silk we performed two types of tests. In some instances, silk threads were restrained at a constant length, which we refer to as 'wetted strained' tests (WS*x*) where '*x*' refers to the strain of the specimen. In other instances, silk threads were not restrained but were subjected to constant loading, which we refer to as 'wetted loaded' tests (WL).

To measure the stress generated by spider silk under changing humidity, individual fibers of major ampullate silk were first collected from restrained *Nephila clavipes* (Linnaeus 1776) and adhered to cardboard mounts across 21 mm gaps, as described previously (Blackledge et al., 2005b). The diameters of fibers were then measured to the nearest 0.1 μm using polarized light microscopy

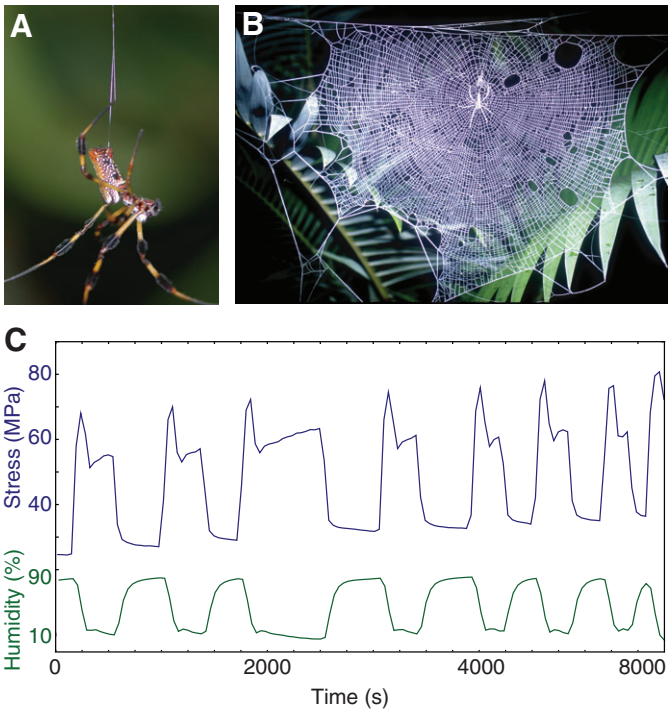

Fig. 1. Cyclic stress response of spider dragline silk to humidity. Spiders use dragline silk both as (A) lifelines and (B) the supporting framework of their webs. (C) Dragline silk repeatedly contracts upon drying and then relaxes upon subsequent wetting. This response is nearly instantaneous and produces large stresses. The spikes in stress at the beginning of each drying cycle are caused by brief puffs of dry N_2 in the environmental chamber before the introduction of small amounts of moisture to control humidity (i.e. the chamber is briefly much drier than can be maintained long term). Although these spikes probably represent the maximum performance of the silk and illustrate how quickly the response occurs, we consider here values measured from the stable plateaus several seconds after the target humidity is achieved.

(Blackledge et al., 2005a) before testing. Measurements of stress were performed using an MTS Nano Bionix that measured force to ±10 μN. The Nano Bionix was custom fit with an environmental chamber that controlled humidity to an accuracy of 1% with a range of ~1–95% RH. Humidity in the environmental chamber was regulated by dividing the flow of dry gaseous N_2 into channels, one of which flowed through a 1 m high water column and the other which remained dry. The controller then mixed the two flows before they entered the chamber, to achieve the desired humidity. The feedback between the hygrometer on the chamber and the controller was slow enough that an initial switch from wetting to drying was usually accomplished through a brief burst of completely dry N_2 that was then rapidly mixed with a small amount of moist gas. This resulted in a brief 'undershooting' of the targeted dryness that normally occurred too quickly to register on the hygrometer, but did manifest itself in some tests (see below). The opposite effect also occurred to a lesser degree during wetting.

Silk was mounted onto the grips of the Nano Bionix at a strain of 0.5%. The chamber was then cycled to ~90% RH to achieve a fully supercontracted state in the fibers. Finally, each silk fiber (N=35) was exposed to approximately eight cycles of humidity while stress was measured continuously. Similar procedures were used to test fibers of polyethylene (N=6), acrylic (N=7), cotton (N=5), keratin (hair, N=7) and both native (N=9) and degummed silkworm (N=16) fibers. For one series of tests, a bundle of 90 fibers of spider silk was used. Fibers were then removed from the bundle and the test repeated until only a single fiber remained.

To measure the capacity of spider silk to perform work, six progressively heavier weights (2–100 mg) were suspended from 30–40 mm long fibers of major ampullate silk that were mounted within the environmental chamber. Weights were constructed from pipette tips and secured using cyanoacrylate adhesive. Clear acetate was used to provide a window in the chamber through which digital photographs were taken using an eight megapixel Nikon D200 camera. For each test, photographs were taken immediately after the chamber reached either high (~90%) or low (~5%) humidity through five to nine cycles. The displacement of the weight was then determined in each photograph using the image analysis software ImageJ (http://rsbweb.nih.gov/ij/) by measuring the length, in pixels, of the silk. Before testing, the diameters of the fibers were measured as described above, the total volume of silk calculated, and silk mass (m) estimated using a density of 1.3 g cm^{-3} (Stauffer et al., 1994). Power (P) was calculated as:

$$P = w/t\,, \tag{1}$$

where w is the work performed and t is the time for displacement to occur. We calculated P using times of both 2 and 3 s, based upon videos of the rate at which supercontraction occurs in unrestrained silk and the response time of restrained silk to changes in humidity (Fig. 1C), respectively. Power density (Pd) was then calculated as:

$$Pd = P/m\,, \tag{2}$$

where m is the estimated mass of the silk fiber. Work density (Wd) was calculated as:

$$Wd = w/v\,, \tag{3}$$

where v is the volume of the silk fiber.

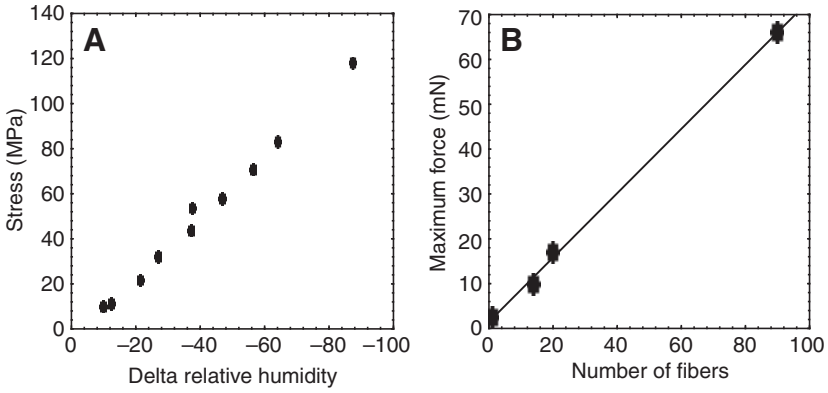

Fig. 2. Scalability of cyclic stress response. (A) Linear increase in stress generated as silk dries. Change in humidity is relative to an initial 95% RH, immediately after fiber supercontraction. (B) Maximum force generated by restrained silk scales linearly with the number of silk fibers bundled together. All fibers were from the same spider and ~4.2 μm diameter.

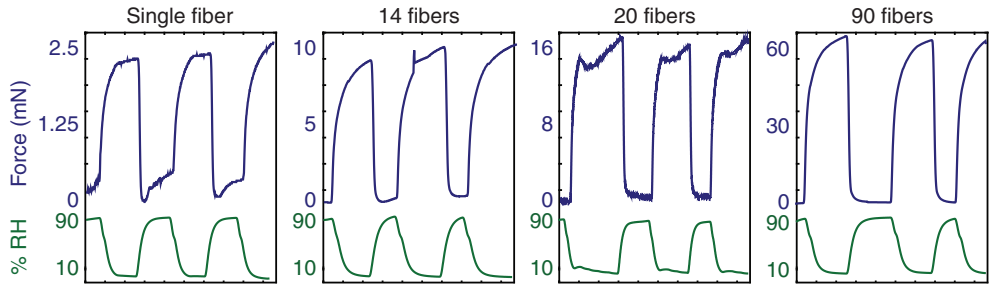

Fig. 3. Contraction force scales linearly with bundle size. Panels illustrate cyclic forces generated by restrained silk for a single 4.2 μm fiber through increasingly larger bundles of fibers (all from the same spider's dragline and approximately the same diameter). Each cycle of humidity occurred over ~10 min.

RESULTS

Fig. 1C shows the response of a single 5 μm diameter dragline thread from the golden silk spider *Nephila clavipes* to cyclical changes in humidity. The test began at high humidity. Initial drying induces stress (contraction) of ~40 MPa (ranging from 10–140 MPa across 35 independent tests). The fiber then relaxes back to its original tension when humidity is subsequently increased. This cyclic response occurs independently of supercontraction, generating high forces in the silk. Fig. 1C shows eight repetitions with no evidence for fatigue in the silk, even after approximately 100 min under tension. The magnitude of the stress generated is directly proportional to the change in humidity (Fig. 2A), providing a precise mechanism to control the stress generated by the spider silk. The total force generated increases as fibers are bundled together (Fig. 2B, Fig. 3).

The cyclic contraction of spider silk can produce work, sufficient for a single ~40 mm long, 5 μm diameter fiber to lift at least 100 mg. Fig. 4 shows cyclic lifting of a 9.5 mg weight in response to seven cycles of drying in an environmental chamber. The work generated as a function of applied stress is shown in Fig. 5. We estimate that the lifting response occurs within 3 s, as indicated by video analysis of the much larger amplitude changes during supercontraction. Also, the maximum change in stress during the WS testing approached 20–30% of the total magnitude per second. This time can probably be reduced further by increasing the rate of change in humidity. Using a 3 s response time, a maximum power density of 130 W kg^{-1} is achieved at a stress of 50 MPa (Table 1). This power density is comparable to human muscles (Kornbluh et al., 1998; Madden et al., 2004). In addition, the maximum sustainable stress of 80 MPa, which defines the upper limit at which silk can no longer perform work, is much higher than the 0.1–0.4 MPa for typical biological muscles. Furthermore, this stress can be maintained for long periods without additional input of energy, in contrast to natural muscle. We also determine that the maximum work density of silk fibers is 500 kJ m^{-3}, 50 times higher than most biological muscles (Kornbluh et al., 1998; Madden et al., 2004). Thus, spider silk rapidly achieves high force at an impressively light weight.

DISCUSSION

The maximum sustainable stress, work density, power density and modulus for silk are superior to many synthetic polymer-based muscle mimics (Table 1). In addition, most successful polymer-based

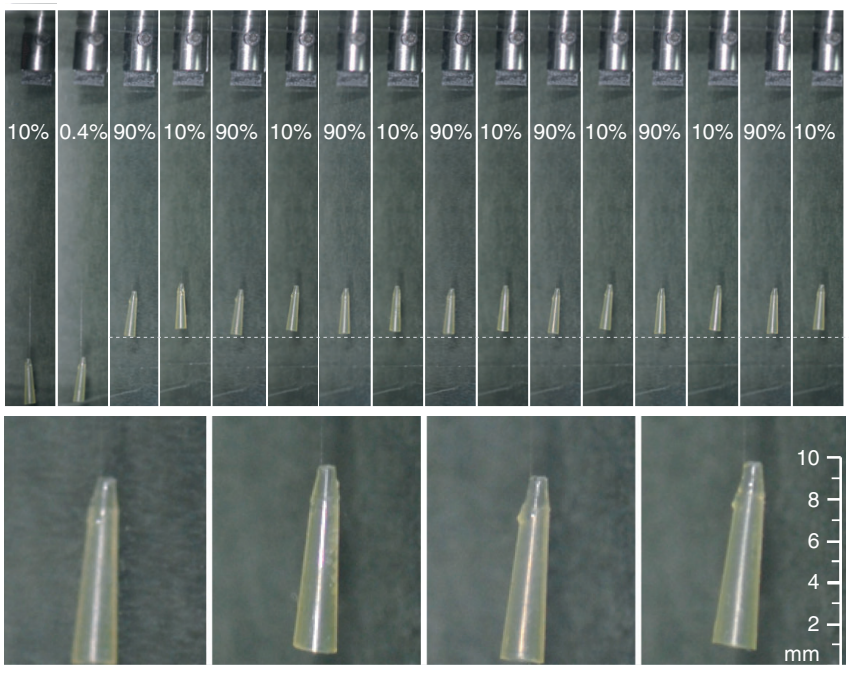

Fig. 4. Lifting performed by spider dragline silk during repeated cycles of wetting and drying. A plastic weight is suspended from a single dragline silk thread and subjected to repeated changes in humidity. The relative humidity is indicated in each frame. The initial increase in humidity results in a large displacement during supercontraction. Subsequently, the single 5.5 μm diameter silk thread repeatedly lifted the 9.5 mg weight through seven cycles of drying. The average displacement during each contraction was 0.65 mm or 1.7% of the thread's total post-supercontraction length (enlarged views for two cycles are shown at the bottom).

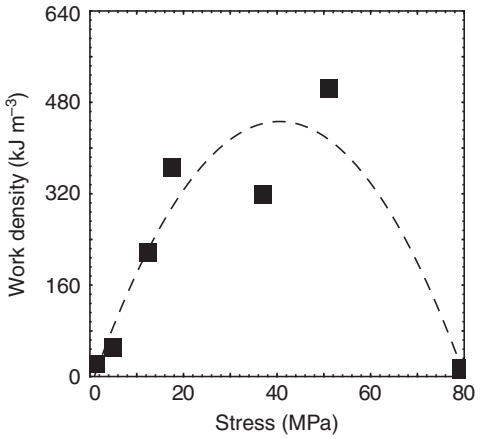

Fig. 5. Work density generated by spider dragline silk as a function of the force (normalized by the cross sectional area) lifted by the fiber (WL tests). The maximum stress data point was obtained from a $WS_{0.5\%}$ test. Strain amplitude generally decreased with increasing stress, but is not shown.

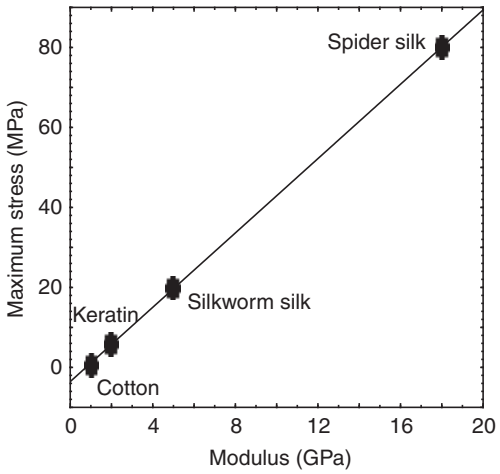

Fig. 6. Maximum stress generated by different hydrophilic materials scales directly with modulus (R^2=0.99).

synthetic muscle mimics are activated by electric fields ($E=V/d$) (Bar-Cohen, 2004; Bar-Cohen et al., 2007; Madden et al., 2004; Osada et al., 1992). In order to keep the driving voltages (V) low, the devices have to have a diameter of ~100–900 μm and many layers have to be stacked together to scale up the devices to larger dimensions (Osada et al., 1992). In comparison, the force lifted by a single silk fiber can be easily scaled up by forming bundles or sheets of silk fibers (Fig. 3). Bundles of 1–90 silk fibers lift forces that scale directly with the number of fibers (Fig. 2B). Extrapolating, we estimate that a silk bundle equivalent in cross-sectional area to a 1 mm diameter fiber could lift as much as 5 kg whereas the equivalent of a 2 cm diameter fiber could lift 2 metric tons, making silk useful for a range of applications from micro-electro-mechanical systems (MEMS) to macro-robotics (e.g. Bar-Cohen, 2003; Shahinpoor et al., 1998).

The main limitation of silk as a biomimetic muscle fiber is the small maximum displacement that can be achieved (maximum strain of 2.5%). In general though, materials that exhibit higher strains have substantially lower sustainable stress and modulus compared with spider silk (Table 1). Moreover, there is considerable variation in silk produced by different species of spiders (Swanson et al., 2006) such that bioprospecting may reveal species whose silk maintains higher cyclic strain without compromising other properties. More importantly, we also observed cyclic contraction in silkworm silk (Fig. 6). Even though the maximum power density for silkworm silk is lower than spider silk, its commercial availability offers the possibility of using large lengths of silk threads. The potential limitation of lower strain can therefore be overcome by using larger lengths of silk or through strain amplification. The use of silk threads, or even two-dimensional woven silk mats, is an attractive technology for lightweight biomimetic muscles. The micron to sub-micron diameters of spider silk fibers results in a high surface to volume ratio that is ideal for fabricating devices controlling application of water through microfluidic geometries (e.g. Sia and Whitesides, 2003; Wheeler and Stroock, 2008).

Our focus here is on the potential applicability of silk as a biomimetic muscle, rather than on the causes of the cyclic contraction itself. However, cyclic contraction is clearly a phenomenon distinct from supercontraction (Blackledge et al., 2009). It is repeatable both before and after supercontraction, and infiltration of water causes the relaxation phase. We hypothesize that water molecules cause a general swelling of the silk and their removal during drying results in contraction. This is strikingly similar to the mechanism proposed to explain how plant tissues can act as motors – actively expelling seeds from the parent plant and even burying seeds in the ground (Dawson et al., 1997; Elbaum et al., 2007). For instance, differential expansion and contraction on opposite sides of the cellulose awns of wheat seeds causes them to bend under daily fluctuations of humidity thereby burying the seeds in the ground (Elbaum et al., 2007). Thus, cyclic contraction of spider silk may result from a relatively general response of biological tissues to humidity. This is supported by our finding of a lack of cyclic contraction in hydrophobic synthetic fibers, such as polyethylene and acrylic, whereas it is weakly exhibited by natural fibers such as cotton and hair (0.6±0.1 and 6.1±3.0 MPa, respectively). Moreover, cyclic contraction occurs in other types of

Table 1. Comparison of natural muscle and spider silk to different polymeric-based synthetic biomimetic muscle materials

	Muscle fiber	Silk fiber	Polyurethane (electrostrictive)‡	Liquid crystal polymers†	Conductive polymers†	Ferroelectric polymers†
Sustainable stress (MPa)	0.1†-0.35‡	80	1.9	0. 45	5–34	20
Work density (kJ m^{-3})	8 (typical)–40 (max)	500	100	3-56	100	300
Power density (W kg^{-1})	50–300	130–190*	–	1	150 (max)	–
Strain (%)	20†, >40‡	2.5	11	19–45	2–12	3.5
Modulus (MPa)	10–60	18000	17	4	800	400
Mechanism	Chemical	Humidity	Voltage	Voltage	Voltage	Voltage

*Power density was calculated using both 3 and 2 s response times.
†Madden et al., 2004; ‡Kornbluh et al., 1998.

silk, such as fibers spun by silkworms (Fig. 6). The stresses generated in all of these materials during humidity cycling scale directly with stiffness. Thus, the impressive capacity of spider silks to perform work probably depends in large part on the high modulus of spider silk (10–20 GPa), the hydrophilic nature of some of its constituent proteins, and the relatively high cyclic strain caused by changes in humidity. Together, these properties combine to generate work density 50× higher than biological muscles.

In summary, we demonstrate the use of dry and wet air to control the contraction and relaxation of spider silk and silkworm fibers. This results in a very environmentally friendly and energy efficient mimic of biological muscles that generates impressive power density. Silk thus emerges as an attractive model for biomimetic muscle fibers that could be used for a range of applications in industry and the biomedical sciences.

We thank Linden Higgins and Claire Ritschoff for supplying spiders. Cecilia Boutry and Victoria Sain assisted with collection of data for non-spider silk fibers. Cheryl Hayashi, Alan Gent, John Gosline, Hans Thewissen, and an anonymous reviewer provided helpful comments on early drafts of the manuscript. This work was supported by National Science Foundation awards DBI-0521261 (T.A.B.), IOS-0745379 (T.A.B.), DEB-0516038 (T.A.B.) and DMR-0512156 (A.D.). Additional funding was provided by a Slovenian Research Agency research fellowship ARRS Z1-9799-0618-07 (I.A.), and from the Integrated Bioscience Program at University of Akron.

REFERENCES

Bar-Cohen, Y. (2003). Actuation of biologically inspired intelligent robotics using artificial muscles. *Ind. Rob.* **30**, 331-337.

Bar-Cohen, Y. (2004). *Electroactive Polymer (EAP) Actuators as Artificial Muscles: Reality, Potential and Challenges*. Bellingham, WA: SPIE Publications.

Bar-Cohen, Y., Kim, K. J., Choi, H. R. and Madden, J. D. W. (2007). Electroactive polymer materials. *Smart Mater. Struct.* **16**, S195-S196.

Beebe, D. J., Moore, J. S., Bauer, J. M., Yu, Q., Liu, R. H., Devadoss, C. and Jo, B. H. (2000). Functional hydrogel structures for autonomous flow control inside microfluidic channels. *Nature* **404**, 588-590.

Bell, F. I., McEwen, I. J. and Viney, C. (2002). Fibre science: Supercontraction stress in wet spider dragline. *Nature* **416**, 37.

Blackledge, T. A., Cardullo, R. A. and Hayashi, C. Y. (2005a). Polarized light microscopy, variability in spider silk diameters, and the mechanical characterization of spider silk. *Invertebr. Biol.* **124**, 165-173.

Blackledge, T. A., Swindeman, J. E. and Hayashi, C. Y. (2005b). Quasistatic and continuous dynamic characterization of the mechanical properties of silk from the cobweb of the black widow spider *Latrodectus hesperus*. *J. Exp. Biol.* **208**, 1937-1949.

Blackledge, T. A., Boutry, C., Wong, S.-C., Baji, A., Dhinojwala, A., Sahni, V. and Agnarsson, I. (2009). How super is supercontraction? Persistent *versus* cyclic responses to humidity in spider dragline silk. *J. Exp. Biol.* **212**, 1981-1989.

Dawson, C., Vincent, J. F. V. and Rocca, A. (1997). How pine cones open. *Nature* **390**, 668.

Elbaum, R., Zaltzman, L., Burgert, I. and Fratzl, P. (2007). The role of wheat awns in the seed dispersal unit. *Science* **316**, 884-886.

Gosline, J. M., Denny, M. W. and Demont, M. E. (1984). Spider silk as rubber. *Nature* **309**, 551-552.

Gosline, J. M., Demont, M. E. and Denny, M. W. (1986). The structure and properties of spider silk. *Endeavour* **10**, 37-43.

Gosline, J. M., Guerette, P. A., Ortlepp, C. S. and Savage, K. N. (1999). The mechanical design of spider silks: from fibroin sequence to mechanical function. *J. Exp. Biol.* **202**, 3295-3303.

Guinea, G. V., Elices, M., Pérez-Rigueiro, J. and Plaza, G. (2003). Self-tightening of spider silk fibers induced by moisture. *Polymer* **44**, 5785-5788.

Hayashi, C. Y., Shipley, N. H. and Lewis, R. V. (1999). Hypotheses that correlate the sequence, structure, and mechanical properties of spider silk proteins. *Int. J. Biol. Macromol.* **24**, 271-275.

Jelinski, L. W., Blye, A., Liivak, O., Michal, C., LaVerde, G., Seidel, A., Shah, N. and Yang, Z. T. (1999). Orientation, structure, wet-spinning, and molecular basis for supercontraction of spider dragline silk. *Int. J. Biol. Macromol.* **24**, 197-201.

Kornbluh, R., Pelrine, R., Eckerle, J. and Joseph, J. (1998). Electrostrictive polymer artificial muscle actuators. *Proc. IEEE Int. Conf. Robot. Autom.* **3**, 2147-2154.

Madden, J. D. W., Vandesteeg, N. A., Anquetil, P. A., Madden, P. G. A., Takshi, A., Pytel, R. Z., Lafontaine, S. R., Wieringa, P. A. and Hunter, I. W. (2004). Artificial muscle technology: physical principles and naval prospects. *IEEE J. Oceanic Eng.* **29**, 706-728.

Osada, Y., Okuzaki, H. and Hori, H. (1992). A polymer gel with electrically driven motility. *Nature* **355**, 242-244.

Schafer, A., Vehoff, T., Glisovic, A. and Salditt, T. (2008). Spider silk softening by water uptake: an AFM study. *Eur. Biophys. J.* **37**, 197-204.

Shahinpoor, M., Bar-Cohen, Y., Simpson, J. O. and Smith, J. (1998). Ionic polymer-metal composites (IPMCs) as biomimetic sensors, actuators and artificial muscles – a review. *Smart Mater. Struct.* **7**, R15-R30.

Sia, S. K. and Whitesides, G. M. (2003). Microfluidic devices fabricated in poly(dimethylsiloxane) for biological studies. *Electrophoresis* **24**, 3563-3576.

Stauffer, S. L., Coguill, S. L. and Lewis, R. V. (1994). Comparison of the physical properties of three silks from *Nephila clavipes* and *Araneus gemmoides*. *J. Arachnol.* **22**, 5-11.

Swanson, B. O., Blackledge, T. A., Summers, A. P. and Hayashi, C. Y. (2006). Spider dragline silk: correlated and mosaic evolution in high performance biological materials. *Evolution* **60**, 2539-2551.

Tanaka, T., Fillmore, D., Sun, S. T., Nishio, I., Swislow, G. and Shah, A. (1980). Phase transition in ionic gels. *Phys. Rev. Lett.* **45**, 1636-1639.

Termonia, Y. (1994). Molecular modeling of spider silk elasticity. *Macromolecules* **27**, 7378-7381.

Vadlamudi, S. (1995). Suitability of spider silks for biomedical applications. MS Thesis, University of Wyoming.

Vollrath, F. and Knight, D. P. (2001). Liquid crystalline spinning of spider silk. *Nature* **410**, 541-548.

Vollrath, F. and Porter, D. (2006). Spider silk as a model biomaterial. *Appl. Phys. A Mater. Sci. Proc.* **82**, 205-212.

Wheeler, T. D. and Stroock, A. D. (2008). The transpiration of water at negative pressures in a synthetic tree. *Nature* **455**, 208-212.

Work, R. W. (1977). Dimensions, birefringences, and force-elongation behavior of major and minor ampullate silk fibers from orb-web-spinning spiders-the effects of wetting on these properties. *Tex. Res. J.* **47**, 650-662.